Calculated ν(TeO) values for $OTeF_5^-$ and $Na^+OTeF_5^-$ are 19 and 100 cm^{-1} higher, respectively, than the experimental value of 867 cm^{-1}, while calculated ν(TeF) values are 30 and 36 cm^{-1} too low for $OTeF_5^-$ and 58 and 33 cm^{-1} too high for $Na^+OTeF_5^-$ when compared with the observed values of 645 and 576 cm^{-1}. The ν(TeF) bands in Raman spectra of $[N(n\text{-}Bu)_4^+][OTeF_5^-]$ shift by 1 cm^{-1} and <1 cm^{-1} upon ^{18}O substitution (see Table IV). Our calculations have overestimated this vibrational coupling: we calculate shifts of 5 and 1 cm^{-1} for $OTeF_5^-$ and 3 and 1 cm^{-1} for $Na^+OTeF_5^-$.

The calculated geometry of the $OTeF_5$ radical is substantially different from that calculated for the teflate anion. The equatorial fluorine atoms that are coplanar with the singly occupied oxygen p orbital distort toward that radical orbital while the other two equatorial fluorine atoms distort away from the doubly occupied oxygen p orbital with which they are coplanar, leaving the $OTeF_5$ radical with only C_{2v} symmetry. On going from the $OTeF_5^-$ anion to the $OTeF_5$ radical, the Te–F distances should shorten by 0.04 Å and the Te–O distance should lengthen by 0.14 Å. For a HF wave function, the calculated electron affinity of the $OTeF_5$ radical is 4.65 eV (cf. TeF_6, 3.10 eV[14]). A vibrational progression of 819 cm^{-1} in the photodetachment spectrum of $OTeF_5^-$ is anticipated due to the substantial difference in TeO distances. The $OTeF_5$ radical has been generated by the photolysis of $Xe(OTeF_5)_2$ and identified by a matrix-isolation EPR experiment,[24] but little else is known about this species.

The molecular orbitals presented in Figures 3–5 demonstrate only a very slight change in Te–O π bonding on going from the $OTeF_5$ radical to the free $OTeF_5^-$ anion (cf. Figure 3b,c with Figure 4b,c). Nevertheless, the Te–O bond strength of the anion is significantly greater than that of the radical, as shown by the shortening of the Te–O distance by 0.14 Å and an increase in ν(TeO) by 67 cm^{-1} on going from the radical to the anion. The difference in net Mullikan charges for these two species (Table VIII) shows that the increased Te–O bond strength of the free anion is due almost entirely to an increased electrostatic interaction between the positively charged tellurium atom and the negatively charged oxygen atom.

We have also calculated the geometry for the triplet excited state of $OTeF_5^-$, which is analogous to the bound state of TeF_6^- (see Figure 5b).[14] This state is achieved by adding an electron to a symmetric tellurium orbital of the $OTeF_5$ radical rather than to the singly occupied p orbital on the oxygen atom (which would produce the singlet state of $OTeF_5^-$). The ground-state-singlet to excited-state-triplet excitation energy, calculated with a restricted HF wave function, is estimated to be ~15 000 cm^{-1}. The excited state has longer Te–O and Te–F bond distances, by 0.14 and 0.11 Å, respectively, relative to the ground state (cf. TeF_6 and TeF_6^-, where the distances differ by 0.11 Å[14]).

Acknowledgment. This research was supported by a grant from the NSF (CHE-8419719). We thank Professors J. R. Norton and A. T. Tu for the use of their IR and Raman spectrometers, respectively, Dr. B. I. Swanson for helpful discussions, and S. A. Ekberg, M. R. Colsman, L. F. Taylor, J. H. Reibenspies, and M. M. Miller for experimental assistance. P.K.M. thanks the Mobay Corp. for a Graduate Student Research Award. K.D.A. acknowledges the support of the Department of Energy. The Nicolet R3m/E diffractometer and computing system were purchased with NSF Grant No. CHE-8103011. Acknowledgment is made to the CSU Supercomputing Project for partial support of this research.

Registry No. $[pyH^+][OTeF_5^-]$, 40904-35-6; $[lutH^+][OTeF_5^-]$, 114595-21-0; $HOTeF_5$, 57458-27-2; $[(PS)H^+][OTeF_5^-]$, 114595-22-1; $H^{18}OTeF_5$, 114595-23-2; CaH_2, 7789-78-8; TeF_6, 7783-80-4; $OTeF_5^-$, 42503-56-0; $Na^+OTeF_5^-$, 53150-40-6; $OTeF_5$, 114595-24-3; $[N(n\text{-}Bu)_4^+][OTeF_5^-]$, 102648-79-3; ^{18}O, 14797-71-8.

Supplementary Material Available: Figure S1, showing a stereoview of the packing of $[(PS)H^+][OTeF_5^-]$, Tables S-I, S-II, and S-III, respectively, listing thermal parameters, derived hydrogen positions, and bond distances and angles for the $(PS)H^+$ cation, and details of the vibrational analysis of the $OTeF_5^-$ anion (12 pages); Table S-IV, listing observed and calculated structure factors (19 pages). Ordering information is given on any current masthead page.

Contribution from the Solid State and Structural Chemistry Unit, Indian Institute of Science, Bangalore-560012, India

Magnetic Susceptibility Studies on Ternary Oxides of Copper(II)†

K. Sreedhar and P. Ganguly*

Received November 12, 1987

The magnetic susceptibilities of a large number of ternary oxides of copper having structural features common to the presently identified phases of high-temperature superconductors have been studied in the temperature range 14–300 K. The systems studied are Ln_2CuO_4 (Ln = La, Pr, Nd, etc.), $Sr_2CuO_2Cl_2$, Bi_2CuO_4, Ca_2CuO_3, Sr_2CuO_3, $SrCuO_2$, $MgCu_2O_3$, $Ba_2Cu_3O_4Cl_2$, $Y_2Cu_2O_5$, Y_2BaCuO_5, $BaCuO_2$, Li_2CuO_2, etc. Cu^{2+} ions take different coordinations, like isolated square planar, square pyramidal or distorted-tetrahedral and octahedral, in these compounds. These compounds also exhibit different varieties of possible magnetic superexchange interactions like 180° or 90° Cu–O–Cu or Cu–O–O–Cu types as well as direct Cu–Cu interactions. Compounds in which there are extended 180° Cu–O–Cu interactions show a low, nearly temperature-independent susceptibility (100×10^{-6} emu/mol). The estimated value of J for the Cu–O–Cu interaction is between 800 and 1500 K in these compounds. Isolated Cu^{2+} ions in which there are no 180° or close to 180° Cu–O–Cu interactions show Curie–Weiss susceptibility behavior. Compounds with only Cu–O–O–Cu interaction show evidence for the onset of antiferromagnetic coupling between 30 and 50 K. The superexchange rules are useful for explaining the qualitative features of the results. The possibility of disproportionation of Cu^{2+} ion when there are short Cu–Cu distances as in Bi_2CuO_4 is discussed. The extended geometry of the copper–oxygen framework seems to be more important than the local geometry around the Cu^{2+} ion in determining the magnetic properties.

Introduction

The experimental developments, since the discovery of high-temperature superconductivity[1-3] in ternary oxide systems of copper with a low-dimensional component, have far outpaced the theoretical understanding.[4,5] Part of the reason for the theoretical

* To whom correspondence should be addressed.

† Contribution No. 487 from the Solid State and Structural Chemistry Unit.

(1) Bednorz, J. G.; Muller, K. A. *Z. Phys. B: Condens. Matter* **1986**, *64*, 189.

(2) Wu, M. K.; Ashburn, J. R.; Torng, C. J.; Hor, P. H.; Meng, R. L.; Gao, L.; Huang, J.; Wang, Y. Q.; Chu, C. W. *Phys. Rev. Lett.* **1987**, *58*, 908.

0020-1669/88/1327-2261$01.50/0

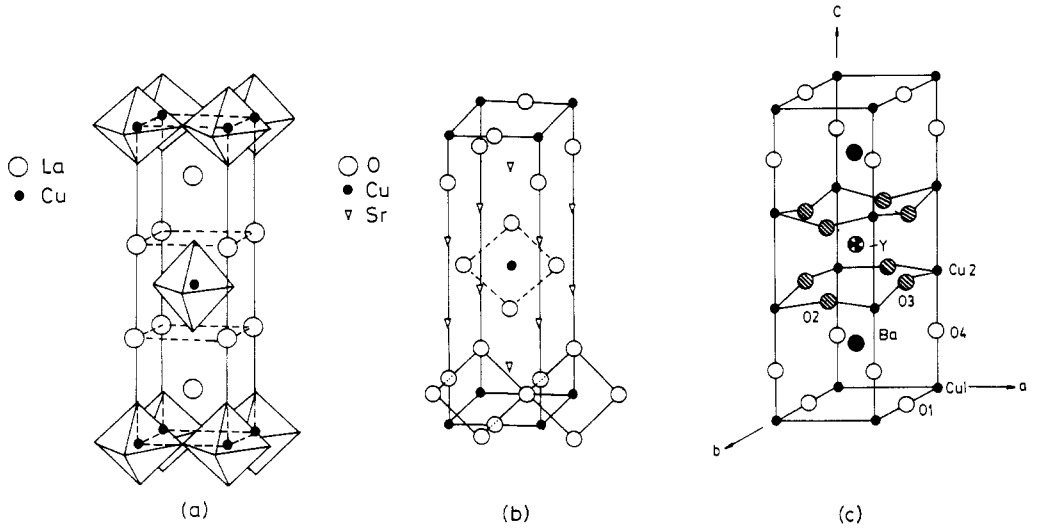

Figure 1. Perspective representation of the relationship between the La_2CuO_4 structure (a) (shown as ideal K_2NiF_4 structural type) to that of Sr_2CuO_3 (b) and a perspective representation of the crystal structure of $YBa_2Cu_3O_7$ (c).

uncertainties is that very little in known about the structure–property correlation in ternary copper oxides, especially with relation to their magnetic properties. One of the attractive theories put forward to explain the high-temperature superconductivity in these oxides is the resonating valence bond theory of Anderson and co-workers.[4] This theory was originally based on the reluctance of the $S = {}^1/_2$ spin system to order antiferromagnetically over a long range. In the transition metal oxides the d electrons are believed to be predominantly responsible for the magnetic and the charge-transport properties. Therefore an intimate relationship is expected between the two. Hence a study of the magnetic properties of the spin $= {}^1/_2$ systems, especially that of oxides containing Cu^{2+} ions (formal charge) would be useful for a better understanding of the superconductivity in ternary copper–oxygen systems.

A large number of compounds with different structural features are known in the ternary copper oxide system.[6,7] The structural features of the superconducting phases (see Figure 1) have been reviewed by Jorgensen.[8] The important structural features of the two superconducting systems are their low dimensionality and the presence of 180° Cu–O–Cu superexchange interaction. In these systems Cu–O–O–Cu interactions as well as direct Cu–Cu interactions are also possible. To understand the relationship between structure and magnetic properties, we have studied the magnetic susceptibility behavior of some model compounds that have at least one of the structural features mentioned above. In addition we have studied some compounds with the following structural features: the CuO_4 square-planar units are isolated; the predominant interactions are of the 90° Cu–O–Cu type; and different types of competing interactions exist, which can lead to frustration in the lattice. We examine in particular the applicability of the superexchange rules[9,10] in predicting the nature of the magnetic interactions. These rules are considered to be applicable in the insulating limit, rather than in the metallic band limit. As yet there is very little work on the magnetic properties[11] of these oxides.

Table I.

compd	starting materials	temp, K	time
$CaCuO_3$	$CaCO_3$; CuO	1300	48 h
Sr_2CuO_3	$Sr(NO_3)_2$; CuO	1300	48 h
$Sr_2CuO_2Cl_2$	$SrCO_3$; $SrCl_2$; CuO	1100	24 h
$Ba_2Cu_3O_4Cl_2$	$BaCO_3$; $BaCl_2$; CuO	1100	24 h
Bi_2CuO_4	Bi_2O_3; CuO	1050	48 h
$La_{1.8}Ba_{1.2}Cu_{0.9}O_{4.8}$	La_2O_3; $Ba(NO_3)_2$; CuO	1300	3 days
$MgCu_2O_3$	$MgCO_3$; CuO	1300	4 days
$BaCuO_2$	$Ba(NO_3)_2$; CuO	1250	48 h
$Y_2Cu_2O_5$	Y_2O_3; CuO	1300	3 days
Li_2CuO_2	$LiOH{\cdot}H_2O$; $Cu(NO_3)_2{\cdot}3H_2O$	900	12 h

Experimental Section

Most of the compounds were synthesized by the ceramic method by taking appropriate molar ratios of the starting materials (~99.9% purity) and heating them in air at the temperatures indicated in Table I with intermittent grinding and pelletizing. Li_2CuO_2 was synthesized by reacting 1:2.5 molar ratios of copper nitrate and lithium hydroxide solutions, and the resulting solution was evaporated to dryness and heated to 900 K for 6 h. $Y_2Cu_2O_5$ was prepared by dissolving appropriate amounts of CuO and Y_2O_3 in nitric acid and decomposing the nitrate mixture at 1300 K. Powder X-ray diffraction patterns of these compounds were recorded to ensure that a single phase of the compound was obtained.

Magnetic susceptibility was measured in the 14–300 K range by the Faraday method using a Cahn-RG electrobalance at a field of 0.43 T. The powder diffraction pattern was obtained on a JEOL JDX-8P X-ray diffractometer. The EPR spectra were recorded by using a Varian E-109 spectrometer operating at X-band.

The oxygen content of all the compounds was determined from thermogravimetric studies of the reduction in hydrogen. Within experimental errors the oxygen content was the same as that expected from the nominal composition in all cases.

Results

180° Cu–O–Cu Interactions. Ln_2CuO_4 (Ln = La, Pr, Nd, Sm, Eu, Gd) and $Sr_2CuO_2Cl_2$. La_2CuO_4 and $Sr_2CuO_2Cl_2$ have a

(3) (a) Uchida, S.; Takagi, H.; Kitazawa, K.; Tanaka, S. *Jpn. J. Appl. Phys.* **1987**, *26*, L1. (b) Takagi, H.; Uchida, S.; Kitazwa, K.; Tanaka, S. *Jpn. J. Appl. Phys.* **1987**, *26*, L123. (c) Chu, C. W.; Hor, P. H.; Meng, R. L.; Gao, L.; Huang, Z. J.; Wang, Y. Q. *Phys. Rev. Lett.* **1987**, *58*, 405. (d) Cava, R. J.; VanDover, R. B.; Batlogg, B.; Rietman, E. A. *Phys. Rev. Lett.* **1987**, *58*, 408. (e) Cava, R. J.; Batlogg, B.; VanDover, R. B.; Murphy, D. W.; Sunshine, S.; Siegrist, T.; Remeika, J. P.; Rietman, E. A.; Zahurak, S.; Espinosa, G. P. *Phys. Rev. Lett.* **1987**, *58*, 1676. (f) Rao, C. N. R.; Ganguly, P.; Raychaudhuri, A. K.; Mohan Ram, R. A.; Sreedhar, K. *Nature (London)* **1987**, *326*, 856. (g) Ganguly, P.; Mohan Ram, R. A.; Sreedhar, K.; Rao, C. N. R. *Pramana* **1987**, *28*, L321.
(4) (a) Anderson, P. W. *Science (Washington, D.C.)* **1987**, *235*, 1196. (b) Baskaran, G.; Anderson P. W., Preprint. (c) Anderson, P. W.; Baskaran, G.; Zou, Z.; Hsu, T. *Phys. Rev. Lett.* **1987**, *58*, 2790. (d) Anderson, P. W. *Mater. Res. Bull.* **1973**, *8*, 153.
(5) (a) Lee, P.; Reed, N. *Phys. Rev. Lett.* **1987**, *58*, 2691. (b) Emery, V. J. *Phys. Rev. Lett.* **1987**, *58*, 2794. (c) Hirsch, J. E. *Phys. Rev. B: Condens. Matter* **1987**, 35, 8726. (d) Mohan, M. M.; Kumar, N. *J. Phys. C* **1987**, *20*, L527. (e) Rice, T. M. *Z. Phys. B: Condens. Matter* **1987**, *67*, 141.
(6) Muller-Buschbaum, H. *Angew. Chem., Int. Ed. Engl.* **1977**, *16*, 674.
(7) Michel, C.; Raveau, B. *Rev. Chim. Miner.* **1984**, *21*, 417.
(8) Jorgensen, J. D. *Jpn. J. Appl. Phys.*, in press.
(9) Anderson, P. W. In *Magnetism*; Rado, G. T., Suhl, H., Eds.; Academic: New York, 1963; Vol. 1, p 25.
(10) Goodenough, J. B. *Prog. Solid State Chem.* **1972**, *5*, 145. Goodenough, J. B. In *Solid State Chemistry*; Rao, C. N. R., Ed., Marcel Dekker: New York, 1973.
(11) Arjumond, M.; Machin, D. J. *J. Chem. Soc., Dalton Trans.* **1975**, 1061.

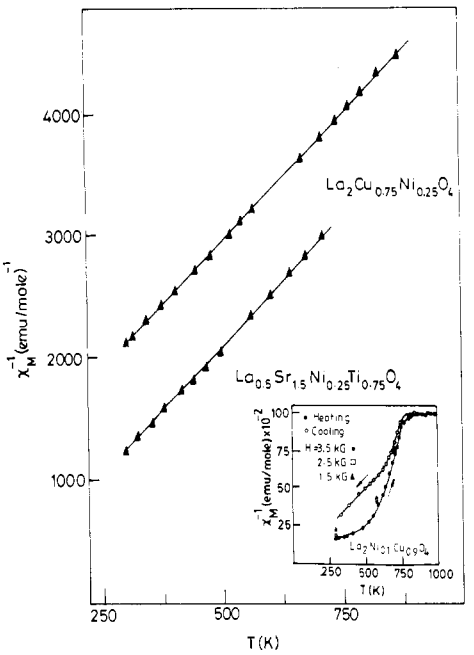

Figure 2. χ_M^{-1} vs T plots ($T > 300$ K) of $La_2Cu_{0.75}Ni_{0.25}O_4$ and $La_{0.5}Sr_{1.5}Ni_{0.25}Ti_{0.75}O_4$. The inset shows a χ_M^{-1} vs T plot of $La_2Cu_{0.9}Ni_{0.1}O_4$ and the field dependence on heating and cooling cycles.

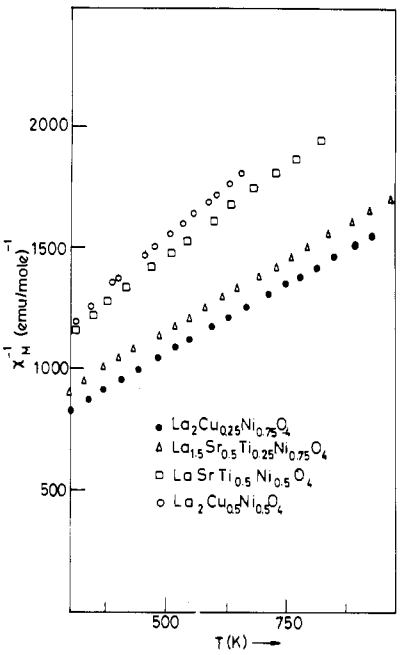

Figure 3. χ_M^{-1} vs T plots (>300 K) of $La_2Ni_{1-x}Cu_xO_4$ and $La_{2-2x}Sr_{2x}Ni_{1-x}Ti_xO_4$.

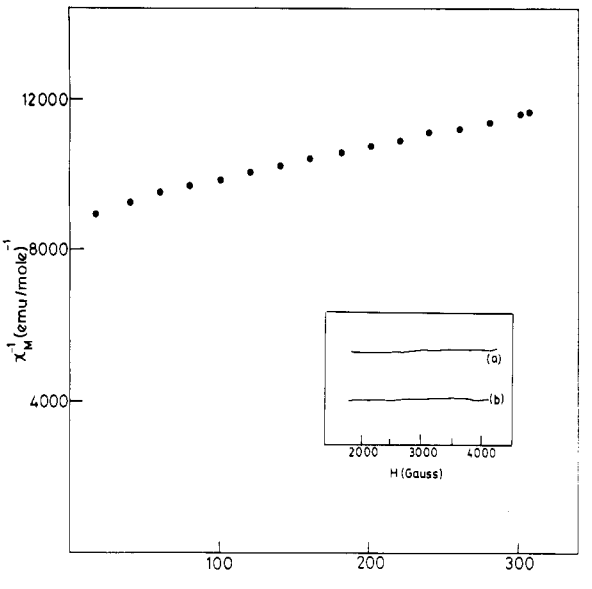

Figure 4. χ_M^{-1} vs T plot of Ca_2CuO_3. The inset shows the ESR spectra of Ca_2CuO_3 (a) and Sr_2CuO_3 (b) at 300 K.

K_2NiF_4-related structure in which the Cu^{2+} ions are in elongated octahedral symmetry[12] (Figure 1a). In the other Ln_2CuO_4 compounds the Cu^{2+} ion takes square-planar coordination.[13] In all these compounds the most dominant interaction is a 180° Cu–O–Cu superexchange interaction. The Cu–O distance in the basal plane varies from 1.90 Å for La_2CuO_4[12] to 1.99 Å for $Sr_2CuO_2Cl_2$.[14]

The magnetic susceptibility of La_2CuO_4 is small[15-17] ($\sim 0.5\ \mu_B$ at 300 K) and shows a large enhancement at low temperatures. The increase in the susceptibility at low temperatures is slower than a $1/T$ increase.[16] The magnetic susceptibility data obtained from this laboratory can be fitted well to a $\chi = C/T^{0.5}$ plot below 200 K. The slope of χ^{-1} vs T plot at high temperature[17,18] gave a value of μ_{eff} close to that expected for an $S = {}^1/_2$ Cu^{2+} ion. A slight maximum is observed around 240 K, which was interpreted[17] in terms of one-dimensional antiferromagnetic ordering. The maximum has been subsequently confirmed[19,20] and has been found by neutron diffraction studies[21,22] to be associated with three-dimensional magnetic ordering. The magnetic susceptibility of insulating La_2CoO_4 also shows[23] a broad maximum in the susceptibility around 550 K followed by another sharp maximum around 400 K. There is always a field dependence in the susceptibility persisting untill high temperatures. The susceptibility of $La_2Ni_{0.1}Cu_{0.9}O_4$ was also found to be strongly field-dependent. The susceptibility at 0.35 T shows a strong hysteresis in the heating and cooling cycles below 800 K (Figure 2, inset). Canted spin antiferromagnets ($LaFeO_3$, for example[9]) with a small ferromagnetic component can show a field dependence in the susceptibility.

The susceptibility of $La_2Ni_{1-x}Cu_xO_4$ is compared with the corresponding compositions of $La_{2-2x}Sr_{2x}Ni_{1-x}Ti_xO_4$ in Figures 2 and 3. The slopes of the χ^{-1} vs T plots at high temperatures are nearly the same. This indicates that even in the isolated square-planar CuO_4 units the Cu^{2+} ion does not show the full moment. The electronic structure of an individual square-planar CuO_4^{6-} cluster has been examined theoretically by Sarma and Sreedhar[24] using spin-polarized MSXα calculations, which indicate the spin polarization on copper in small, supporting the above experimental result. A second possibility is that the Cu and Ni ions are segregated in different layers in the structure, the layer associated with the copper ions remaining magnetically ordered

(12) (a) Longo, J. M.; Raccah, P. M. *J. Solid State Chem.* **1973**, *6*, 526. (b) Grande, B.; Muller-Buschbaum, H.; Schweizer, M. *Z. Anorg. Allg. Chem.* **1977**, *428*, 120.
(13) Muller-Buschbaum, H.; Wollschlager *Z. Anorg. Allg. Chem.* **1975**, *417*, 76.
(14) Grande, B.; Muller-Buschbaum, H. *Z. Anorg. Allg. Chem.* **1975**, *417*, 68.
(15) Ganguly, P.; Rao, C. N. R.; *J. Solid State Chem.* **1984**, *53*, 193.
(16) Singh, K. K.; Ganguly, P.; Goodenough, J. B.; *J. Solid State Chem.* **1984**, *52*, 254.
(17) Ganguly, P.; Kollali, S.; Rao, C. N. R.; Kern, S.; *Magn. Lett.* **1980**, *1*, 107.
(18) Ganguly, P., Unpublished results.
(19) Uchida, S.; Takagi, H.; Yanagisawa, H.; Kishio, K.; Kitazawa, K.; Fueki, K.; Tanaka, S. *Jpn. J. Appl. Phys.* **1987**, *26*, L445.
(20) Fujita, T., Aoki, Y.; Maeno, Y.; Sukurai, J.; Fukuba, H.; Fujii, H. *Jpn. J. Appl. Phys.* **1987**, *26*, L368.
(21) Jorgensen, J. D.; Schuttler, H.-B.; Hinks, D. G.; Capone, D. W., II; Zhang, K.; Brodsky, M. B.; Scalapino, D. J. *Phys. Rev. Lett.* **1987**, *58*, 1024.
(22) Vaknin, D.; Sinha, S. K.; Moncton, D. E.; Johnston, D. C.; Newsam, J.; Safinya, C. R.; King, H. E., Jr. *Phys. Rev. Lett.*, in press.
(23) Ganguly, P.; Ramasesha, S. *Magn. Lett.* **1980**, *1*, 131.
(24) Sarma, D. D.; Sreedhar, K. *Z. Phys. B: Condens. Matter* **1988**, *69*, 529.

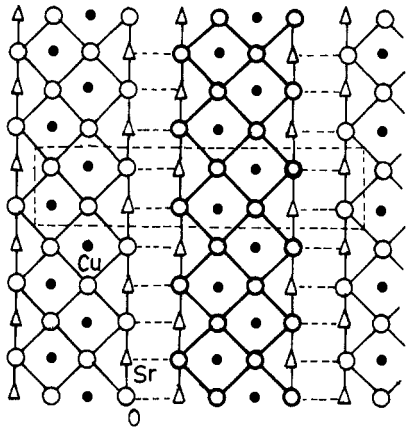

Figure 5. Structure of $SrCuO_2$ projected along [100]. (Reprinted with permission from ref 29. Copyright 1970 Barth.)

untill high temperatures are reached.

The other Ln_2CuO_4 compounds also show very small contributions to the susceptibility from the copper ions[17] at low temperatures. This may be interpreted in terms of antiferromagnetic ordering of the Cu^{2+} ions.[25] Nd_2CuO_4 shows a low satellite intensity in the Cu 2p XPS core signal.[26] Such a reduction in the satellite intensity generally indicates a reduction in the number of unpaired electrons on Cu^{2+} due to strong hybridization with the oxide ligands.

The magnetic susceptibility of $Sr_2CuO_2Cl_2$ has been studied by us. This compound also shows nearly temperature independent low susceptibility (80×10^{-6} emu/mol). Under the ambient humid conditions this compound gets hydrolyzed. Sufficient precautions have to be taken to prevent such an hydrolysis. A small Curie-like contribution to the susceptibility at low temperatures (Curie constant <0.015 emu K^{-1} mol^{-1}) may be attributed to the hydrolysis. However, such a feature has also been obtained in $La_{2-x}Sr_xCuO_{4-(n/2)+\delta}$ ($n > 0.5$) compounds. This is being further investigated.

Ca_2CuO_3, Sr_2CuO_3, and $SrCuO_2$. Ca_2CuO_3 and Sr_2CuO_3 have a structure[27,28] in which there is extended one-dimensional 180° Cu–O–Cu interaction. Magnetic susceptibility of Ca_2CuO_3 is shown in Figure 4. The susceptibility behavior of freshly prepared Sr_2CuO_3 is similar. The susceptibilities of Ca_2CuO_3, Sr_2CuO_3, and $SrCuO_2$ show the absence of any sizable contribution to the magnetic susceptibility from the copper ions. The low magnetic susceptibility is consistent with the very low intensities of their EPR signals. (Figure 4, inset). $SrCuO_2$ has a structure[29] (Figure 5) in which there exists strong one-dimensional Cu–O–Cu interactions along one chain. There is actually a pair of such chains that are coupled together in such a manner that there is 90° Cu–O–Cu interaction between pairs of copper ions in the two chains. Just as in the other compounds with 180° Cu–O–Cu interactions $SrCuO_2$ also shows a very small and weakly temperature-dependent susceptibility (100×10^{-6} emu/mol) indicative of a high antiferromagnetic ordering temperature.

$Ba_2Cu_3O_4Cl_2$. The structure of $Ba_2Cu_3O_4Cl_2$[30] is shown in Figure 6a. Two types of copper sites, Cu_A and Cu_B, can be distinguished in the figure. The Cu_A ions constitute two-thirds of the total number of copper ions, all of which have square-planar coordination with four oxide ions in the basal plane and two chloride ions at the apice of the octahedra, which serve as links

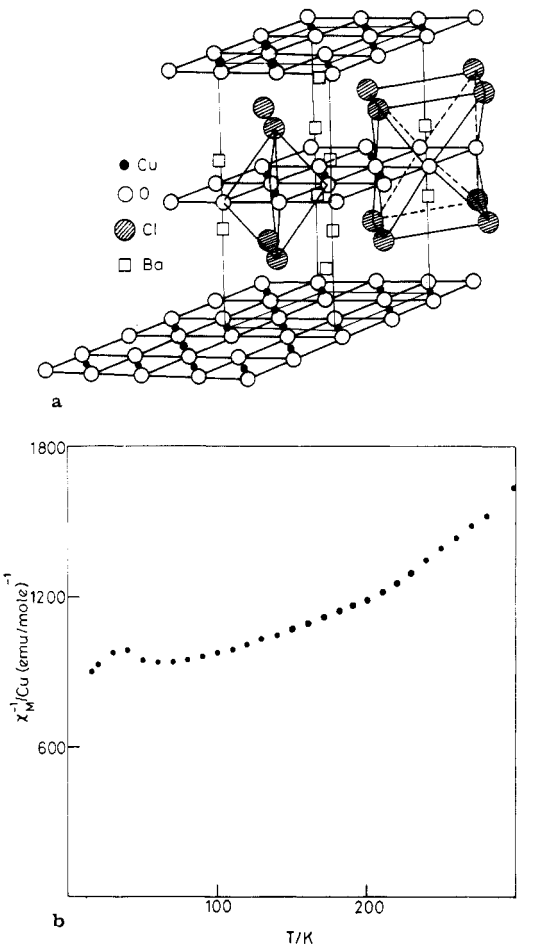

Figure 6. (a) Perspective representation of the crystal structure of $Ba_2Cu_3O_4Cl_2$. (Reprinted with permission from ref 30. Copyright 1976 Barth.) (b) Inverse molar susceptibility per gram atom of copper vs temperature plot of $Ba_2Cu_3O_4Cl_2$.

between the Cu_A ions in different planes. The other one-third of the copper ions (the Cu_B ions) have only square-planar coordination. The Cu_A–O–Cu_A angle is 180° while the Cu_A–O–Cu_B angle is 90°. There are no 180° Cu–O–Cu interactions involving Cu_B ions. The magnetic susceptibility of $Ba_2Cu_3O_4Cl_2$ is shown in Figure 6b. The slope of the χ^{-1} vs T plot gives a C value of 0.20 (emu/K)/g atom of Cu between 150 and 300 K. The slope decreases as the temperature increases, indicating that the Curie constant C may reach the expected value of 0.37 emu/K at higher temperatures.

Bi_2CuO_4. In this compound the Cu^{2+} ions are in an isolated square-planar environment of oxide ions which are stacked one on top of the other in a staggered manner along the c axis (Figure 7a). This gives rise to a one-dimensional array of Cu^{2+} ions with no intervening oxide ions. Cation–anion–cation interactions do not exist in this structure. Superexchange interactions involving two anions are, however, possible both in the a–b plane and along the c axis. The details of the crystal structure do not seem to have been unambiguously resolved. According to Arpe and Muller-Buschbaum[31] the compound has an $I4$ space group with two distinguishable copper sites. A second structure having the space group $P4/ncc$ with only one unique Cu site has also been proposed.[32] An $I4$ symmetry would support the existence of alternating antiferomagnetic chains. A $P4/ncc$ symmetry would support the existence of a uniform antiferromagnetic chain.

The magnetic susceptibility of Bi_2CuO_4 is shown in Figure 7b. There is a marked maximum in the susceptibility around 50 K followed by a minimum around 20 K. Earlier studies[33] between

(25) Saez Puche, R.; Norten, M.; Glaunsinger, W. S. *Mater. Res. Bull.* **1982**, *17*, 1429.
(26) Ganguly, P. *Proc.—Indian Natl. Sci. Acad., Part A* **1986**, *52A*, 135.
(27) Teske, C.; Muller-Buschbaum, H. *Z. Anorg. Allg. Chem.* **1969**, *371*, 325.
(28) Teske, C.; Muller-Buschbaum, H. *Z. Anorg. Allg. Chem.* **1970**, *379*, 234.
(29) Muller-Buschbaum, H.; Mattausch, H. *Z. Anorg. Allg. Chem.* **1970**, *377*, 144.
(30) Kipka, R.; Muller-Buschbaum, H. *Z. Anorg. Allg. Chem.* **1976**, *419*, 58.
(31) Arpe, R.; Muller-Buschbaum, H. *Z. Anorg. Allg. Chem.* **1976**, *426*, 1.
(32) Boivin, J. C.; Thomas, D.; Tridot, G. *C. R. Seances Acad. Sci., Ser. C.* **1973**, 276.

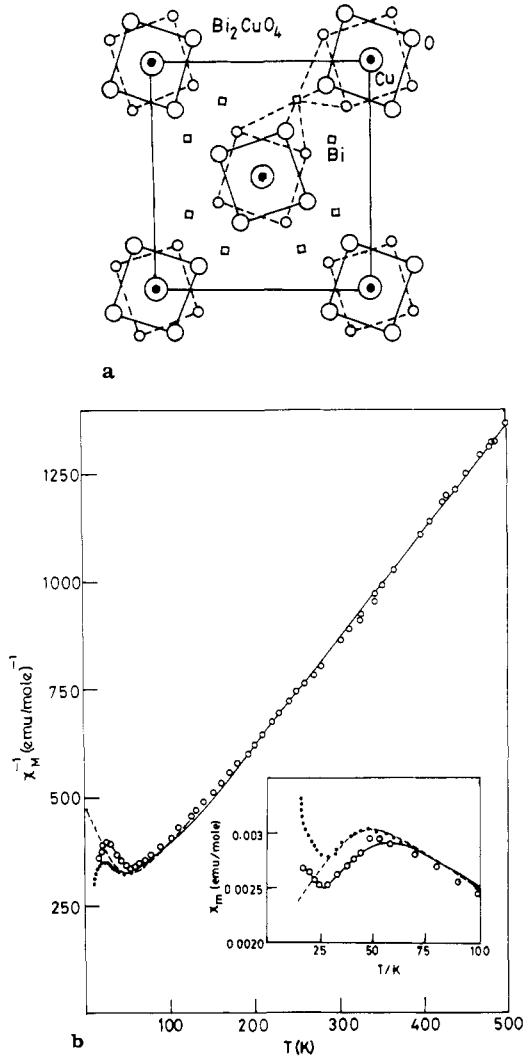

Figure 7. (a) Characteristic arrangement of square-planar CuO_4 polyhedra in Bi_2CuO_4 projected along [001]. (Reprinted with permission from ref 31. Copyright 1976 Barth.) (b) χ_M^{-1} vs T plot of Bi_2CuO_4: circles, experimental points; dashed line, calculated values for infinite chain $S = {}^1/_2$ Heisenberg antiferromagnet;[34] dotted line, mean of chains of 9 and 11 spins;[34] full line, fit with eq 2, with $C' = 0.042$ emu K^{-1} mol^{-1}, $C = 0.57$ emu K^{-1} mol^{-1}, and $2J/k = 100.2$ K. The inset shows χT vs T plots in the range 15–100 K for all of the above cases.

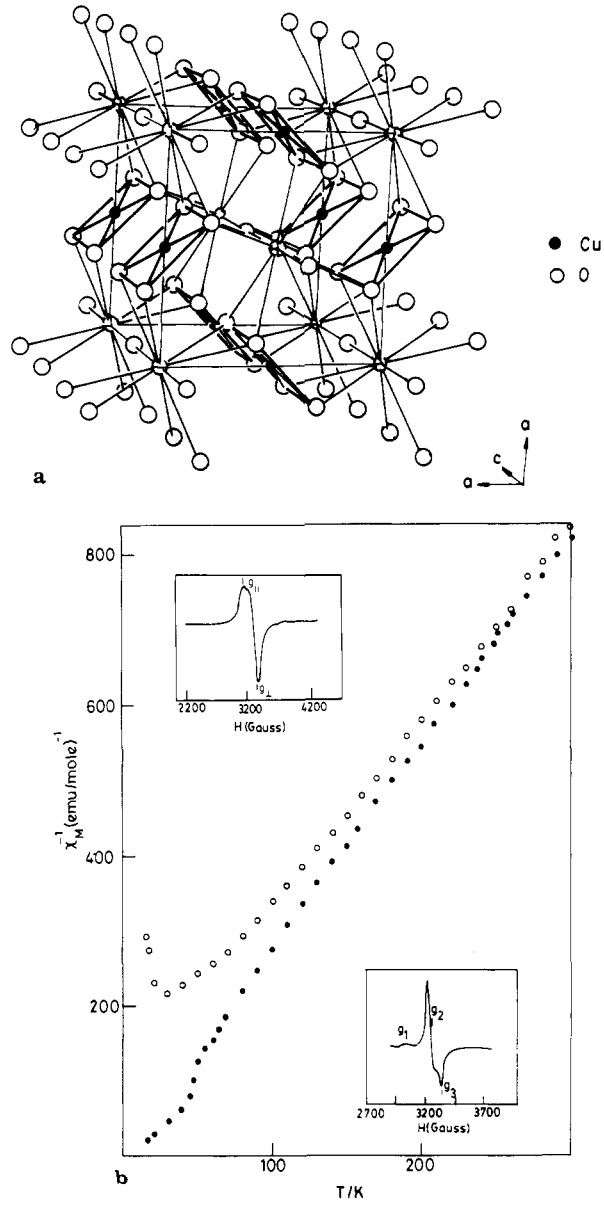

Figure 8. (a) Perspective representation of the crystal structure of Y_2BaCuO_5. (b) Inverse molar susceptibility per gram atom of copper vs temperature plot of Y_2BaCuO_5 (open circle) and $La_{1.8}Ba_{1.2}Cu_{0.9}O_{4.8}$ (closed circle). The inset shows the ESR spectra of Y_2BaCuO_5 (top) and $La_{1.8}Ba_{1.2}Cu_{0.9}O_{4.8}$ (bottom) at 300 K.

77 and 500 K had shown a μ_{eff} of 1.73 μ_B, which is the spin-only value of Cu^{2+}. The ESR of this compound shows a single broad line with a g value of 2.09 over the temperature range 77–500 K, which should yield a μ_{eff} of 1.80 μ_B. The best fit to the Curie–Weiss law at high temperatures indeed gives a μ_{eff} close to 1.80 μ_B. The extrapolated value of the paramagnetic Curie temperature, obtained from the high temperature ($T > 250$K) fit of the data to a Curie–Weiss plot, yields $J/k = 40 \pm 1$ K. The temperature at which the susceptibility shows a maximum, $T(\chi_{max})$ is 50 K. From the Bonner and Fisher model[34] for the uniform $S = {}^1/_2$ Heisenberg antiferromagnetic chain, $kT(\chi_{max})/J = 1.282$ from which we obtain $J/k = 39$ K. This is close to that observed experimentally. Using this value of J/k, we obtain an experimental value of $\chi_{max}J/Ng^2\mu_B{}^2 = 0.0726$, which also compares well with the theoretically predicted value[34] of 0.0734. Thus the high-temperature data point to uniform isotropic spin = ${}^1/_2$ chains, which is consistent with P4/*ncc* symmetry. At low temperatures, however, there is significant deviation from the theoretically predicted curve[34] for uniform Heisenberg spin = ${}^1/_2$ chains, as shown in Figure 7b. This brings up the possibility of the maximum signifying a three-dimensional antiferromagnetic ordering with the interchain interactions being close to the intrachain interactions. The second possibility is that of a spin-Peierls transition.[35,36] Detailed neutron diffraction study may be necessary to examine the low-temperature behavior.

In the limiting case of a spin-Peierls dimerization, the spin-chain breaks up into dimeric units with an excited triplet state separated from the ground-state singlet by a temperature-invariant gap. This picture would be consistent with $I4$ symmetry. The classical Bleaney–Bowers expression[37] for the susceptibility for the dimer as a function of temperature

$$\chi = (C/T)[1 + (1/3)\exp(2J/kT)]^{-1} \qquad (1)$$

gives a very poor fit to the experimental data. However, a good fit is obtained with

(33) Kakhan, B. G.; Lazarev, V. B.; Shaplygin, I. S.; Ellert, O. G. *Russ. J. Inorg. Chem.* (*Engl. Transl.*) **1981**, 26, 124.
(34) Bonner, J. C.; Fisher, M. E. *Phys. Rev. A* **1964**, *135*, 640.
(35) Buzdin, A. I.; Balaerskii, L. N. *Sov. Phys.—Usp.* (*Engl. Transl.*) **1980**, *23*, 409.
(36) Bray, J. W.; Intenante, L. V.; Jacobs, I. S.; Bonner, J. C. In *Extended Linear Chain Compounds*; Miller, J. C. Ed., Plenum: New York, 1982; p 353.
(37) Bleaney, B.; Bowers, K. D. *Proc. R. Soc. London, A* **1952**, *214*, 451.

$$\chi = C'/T + (C/T)[1 + (2/3)\exp(2J/kT)]^{-1} \quad (2)$$

as shown in Figure 7b with $2J/k = 100$ K, $C' = 0.042$ emu/K, and $C = 0.57$ emu/K, respectively. The factor $^2/_3$ in the denominator of eq 2 is the main difference from eq 1. This suggests that there are two singlet states lying close together as the lowest states. The possible significance of this result is discussed below.

Y_2BaCuO_5 and $La_{1.8}Ba_{1.2}Cu_{0.9}O_{4.8}$. As in Bi_2CuO_4, in these compounds the Cu^{2+} ions are isolated[38,39] with no Cu–O–Cu interactions. In Y_2BaCuO_5 the copper ions have a square-pyramidal symmetry, which is shown in Figure 8a. The Cu–O distance to the apex oxygen is large compared with the Cu–O distance in the basal plane. The coordination geometry around the copper ions is close to that of the Cu_2 ions (Figure 1c) in $YBa_2Cu_3O_7$. In Y_2BaCuO_5 these units are connected to one another through Cu–O–O–Cu linkages, the shortest of these being along the c axis. The χ^{-1} vs T plot (Figure 8b) of Y_2BaCuO_5 shows a Curie-like behavior at high temperatures as expected for isolated Cu^{2+} ions. The μ_{eff} value calculated from the slope at high temperatures is 1.73 μ_B, which is the expected spin-only value. The ESR spectrum of this compound is axially symmetric (see Figure 8b, inset) with $g_\perp = 2.08$ and $g_\parallel = 2.22$, which are close to the values reported earlier.[40] The decrease in the susceptibility at low temperatures (30 K) suggests the onset of antiferromagnetic coupling. The temperature at which the maximum occurs (30 K) is close to that recently found[41] in a study of the magnetic susceptibility of a mixed-phase superconducting Y–Ba–Cu–O system.

Michel et al. have reported[39] that the La compounds are stable in the composition range given by $La_{4-2x}Ba_{2+2x}Cu_{2-x}O_{10-2x}$ with $0.15 \leq x \leq 0.25$. We have prepared the composition corresponding to $x = 0.2$. In this compound the Cu^{2+} ions are believed to be in a square-planar geometry. The ESR of this compound is shown in Figure 8b inset. The ESR spectrum at 300 K seems to show features expected for copper ions in compressed octahedra, rather than in a square-planar geometry. However, at low temperatures, it shows a weak line at $g = 2.23$ and the ESR spectrum is best interpreted in terms of an orthorhombic distortion with g_1, g_2, and $g_3 = 2.23$, 2.10, and 2.03, respectively. The χ^{-1} vs T plot is shown in Figure 8b. The value of μ_{eff} calculated per gram atom of copper at high temperatures is 1.70 μ_B, which is close to the spin-only value expected for Cu^{2+} ions. The magnetic susceptibility shows a sharp increase around 40 K, and a weak ferromagnetic component develops below this temperature. Such a behavior is typical of antiferromagnetic ordering with canting of spins, which may be supported in orthorhombic symmetry.

$Y_2Cu_2O_5$. The Cu^{2+} ions in this compounds have a distorted tetrahedral coordination. The structure proposed by Freund et al.[42] is shown in Figure 9a. The structure may be visualized in term of pairs of edge-shared CuO_4 units, these pairs being linked in turn by corners of these units. The Cu–O distances in these units are the shortest. The edge-shared units give rise to 90° Cu–O–Cu interactions. The corner-shared Cu–O–Cu angle, however, is not 180° as it would have been in the ideal structure. Between the chains there is a long Cu–O linkage (~2.30 Å). The interchain Cu–O–Cu angle is also far different from 180°.

The χ^{-1} vs T plot of this compound is shown in Figure 9b. The μ_{eff} value calculated from the slope at high temperatures is nearly 2.00 μ_B. At high temperatures there is a ferromagnetic intercept of the extrapolated χ^{-1} vs T plot, but the susceptibility does not diverge at the lowest temperatures. The high value of μ_{eff} suggests the presence of dimer with a triplet ground state. The Cu^{2+} ions in the two edge-shared CuO_4 units can couple ferromagnetically

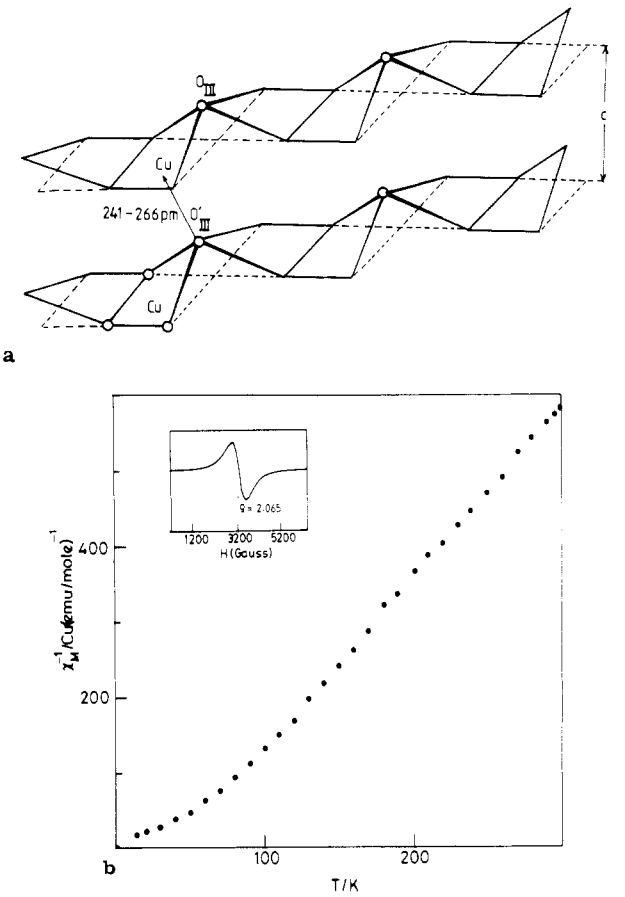

Figure 9. (a) Perspective representation of the crystal structure of $Y_2Cu_2O_5$. (Reprinted with permission from ref 42a. Copyright 1978 Barth.) (b) Inverse molar susceptibility per gram atom of copper vs temperature plot of $Y_2Cu_2O_5$. The inset shows the ESR spectrum of $Y_2Cu_2O_5$ at 300 K.

to produce dimers with $S = 1$. At low temperatures antiferromagnetic interactions seem to become important. In this sense $Y_2Cu_2O_5$ is attractive because of the possibility of the existence of linear chains of antiferromagnetically coupled $S = 1$ dimers.

The ESR spectrum of this compound shows a single, fairly sharp line with g_{iso} nearly equal to 2.065 (see inset of Figure 9b), which is not typical of the ESR of $S = 1$ dimers of Cu^{2+} ions. The ESR results are being further investigated.

$MgCu_2O_3$. The structure[43] of $MgCu_2O_3$ is shown in Figure 10a. The structure is derived from the rock salt structure. The Cu^{2+} ions are in elongated octahedra. The 180° Cu–O–Cu interactions involve long Cu–O bonds. The 90° Cu–O–Cu interactions involve one long and one short bond. The magnetic susceptibility of this compound is shown in Figure 10b. The χ^{-1} vs T plot is concave to the temperature axis. The susceptibility of this compound is expressed fairly well by a relation of the type $\chi = (C/T^\beta)$ with $C = 0.05$ and $\beta = 0.75$. A similar fit has been observed in amorphous antiferromagnets and has been explained[44] in terms of hierarchical condensation of spins.

Li_2CuO_2. This compound has an extremely interesting structure[45] because of the presence of nearly perfect one-dimensional chains of edge-shared square-planar CuO_4 units with only 90° Cu–O–Cu interactions (Figure 11a). The Cu–O distance in the compound is 1.96 Å. This compound should therefore be an ideal candidate for one-dimensional ferromagnetism arising from 90° Cu–O–Cu superexchange interactions involving orthogonal orbitals. The Cu–Cu distance in this compound is 2.84 Å compared to 2.55 Å in metallic copper and 2.92 Å in Bi_2CuO_4. The magnetic

(38) Michel, C.; Raveau, B. *J. Solid State Chem.* **1982**, *43*, 73.
(39) Michel, C.; Er-Rakho, L.; Raveau, B. *Rev. Chim. Miner.* **1984**, *21*, 85.
(40) Michel, C.; Raveau, B., *J. Solid State Chem.* **1983**, *49*, 150.
(41) Sun, J. Z.; Webb, D. J.; Naito, M.; Char, K.; Hahn, M. R.; Hsu, J. W. P.; Kent, A. D.; Mitzi, D. B.; Oh, B.; Beasley, M. R.; Geballe, T. H.; Hammond, R. H.; Kapatulnik, A. *Phys. Rev. Lett.* **1987**, *58*, 1574.
(42) (a) Freund, H. R.; Muller-Buschbaum, H. *Z. Anorg. Allg. Chem.* **1978**, *441*, 103. (b) Bergerhoff, G.; Kasper, H. *Acta Crystallogr., Sect. B: Struct. Crystallogr. Cryst. Chem.* **1968**, *B24*, 388.
(43) Drenkhahn, H.; Muller-Buschbaum, H. *Z. Anorg. Allg. Chem.* **1975**, *418*, 116.
(44) Bhatt, R. N.; Lee, P. A. *J. Appl. Phys.* **1982**, *52*, 703.
(45) Hoppe, R.; Rieck, H. *Z. Anorg. Allg. Chem.* **1970**, *379*, 157.

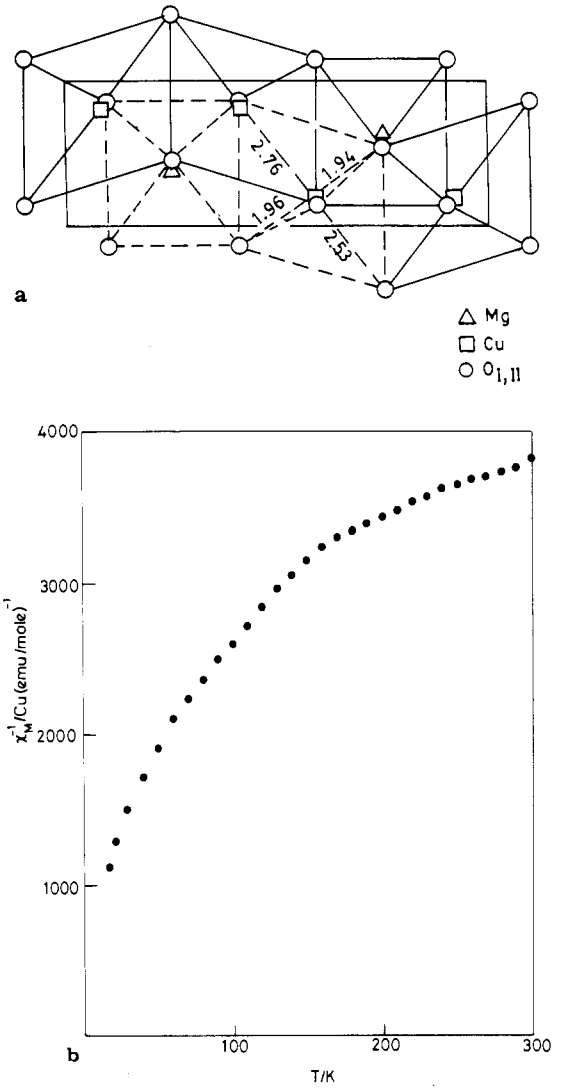

Figure 10. (a) Perspective representation of the crystal structure of $MgCu_2O_3$. The characteristic polyhedra around Cu^{2+} is emphasized. The distances are given in angstrom units. (Reprinted with permission from ref 43. Copyright 1975 Barth.) (b) Inverse molar susceptibility per gram atom of copper vs temperature plot of $MgCu_2O_3$.

susceptibility behavior of this compound as a function of temperature is shown in Figure 11b. The χ^{-1} vs T plot gives a negative value of Θ, indicative of only antiferromagnetic interactions. The slope of this plot gives a μ_{eff} close to that expected for an $S = {}^1/_2$ system.

$BaCuO_2$. The structure[46] and magnetic susceptibility of $BaCuO_2$ are shown in Figures 12 and 11b, respectively. At high temperatures there seems to be a ferromagnetic intercept of the χ^{-1} vs T plot, the slope of which gives a μ_{eff} close to 1.9 μ_B. Just as in $Y_2Cu_2O_5$, the susceptibility does not diverge at the lowest temperatures. There is a large anomaly in the susceptibility around 80 K. The origin of this anomaly is not clear to us as yet.

Discussion

The above results indicate certain systematics that can be explained qualitatively, in most cases, in terms of the semiempirical superexchange rules.[9,10] In square-planar coordination the Cu^{2+} ion has its hole located in the $d_{x^2-y^2}$ orbital. The 180° Cu–O–Cu interaction would therefore involve nonorthogonal cation and anion orbitals and hance should be antiferromagnetic in nature. In $KCuF_3$ the Cu–F–Cu exchange interaction strength has been estimated[47] as $J/k = -190$ K. Compared to that in Fluorides,

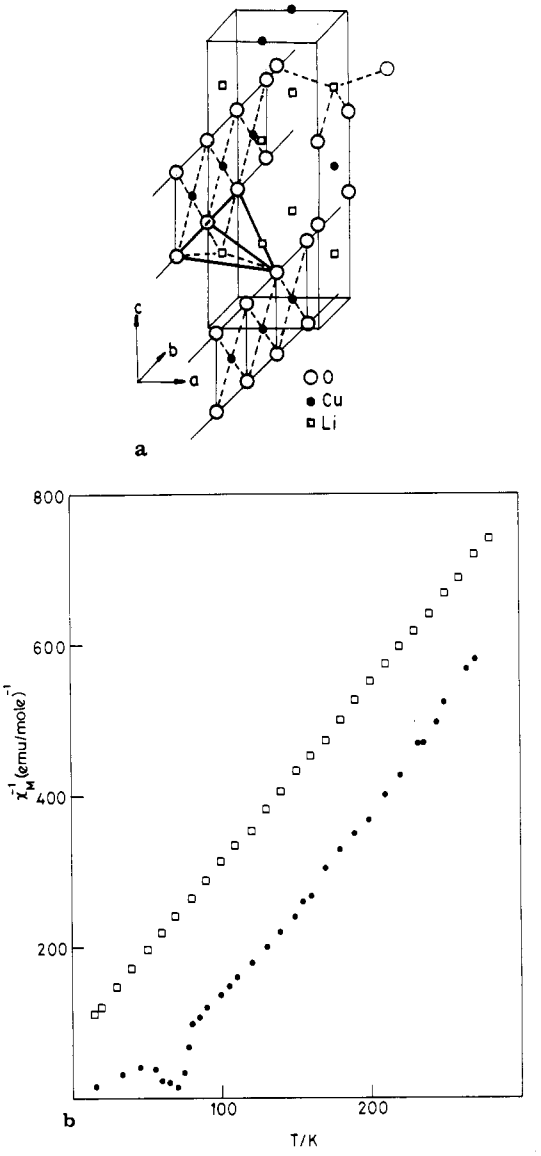

Figure 11. (a) Perspective representation of the extended chains of square-planar CuO_4 units in Li_2CuO_2. The tetrahedral coordination of Li^+ is indicated. (Reprinted with permission from ref 45. Copyright 1970 Barth.) (b) χ_M^{-1} vs T plots for $BaCuO_2$ (circles) and Li_2CuO_2 (squares).

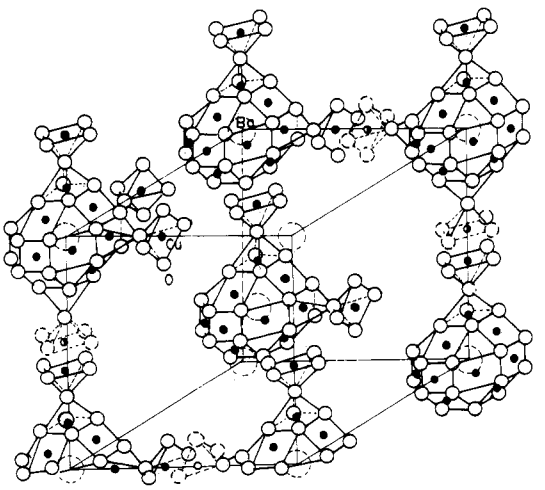

Figure 12. Perspective representation of the crystal structure of $BaCuO_2$. (Reprinted with permission from ref 46. Copyright 1977 Verlag der Zeitschrift für Naturforschung.)

the cation–anion overlap integral is expected to be higher in oxides. The antiferromagnetic ordering temperature of CrF_3 or FeF_3 is

(46) Kipka, R.; Muller-Buschbaum, H. *Z. Naturforsch., B: Anorg. Chem., Org. Chem.* **1977**, *32B*, 121.
(47) deJongh, L. J.; Miedema, A. R. *Adv. Phys.* **1974**, *23*, 1.

nearly two to three times less[48] than that of the corresponding perovskites $LaCrO_3$ and $LaFeO_3$. The antiferromagnetic transition temperature for compounds with 180° Cu–O–Cu interactions is therefore expected to be higher than room temperature.

In terms of mean-field theories, the powder susceptibility below the antiferromagnetic ordering temperature (T_N) is[49] $C/3T_N$ at $T = 0$ K. Assuming $C = 0.375$ emu/K, a susceptibility ($T \rightarrow 0$ K) of (100–200) $\times 10^{-6}$ emu/mol, as found in the compounds with 180° Cu–O–Cu interactions, would suggest that T_N is on the order of 1250–600 K. Such high antiferromagnetic correlation would favor the formation of tightly coupled electron pairs.

Comparison of the magnetic susceptibility of Pr_2CuO_4 and Nd_2CuO_4 with that of $PrAlO_3$ or $NdAlO_3$ enables us to estimate the contribution to the susceptibility from the rare-earth-metal ions. Subtracting out the contribution to the susceptibility from rare-earth-metal ions, we find that the susceptibility of Cu^{2+} ions Pr_2CuO_4 and Nd_2CuO_4 shows a markedly enhanced contribution around 500–600 K. The break in the log χ vs $1/T$ plot in these compounds[50] around 600 K may then be interpreted in terms of effects due to a magnetic order–disorder transition as observed in NiO.[51] The Cu–O–Cu distance in Nd_2CuO_4 (3.95 Å) is comparable to the Cu_2–O–Cu_2 distance in $YBa_2Cu_3O_7$. One may expect, therefore, that in the Cu_2 plane the antiferromagnetic ordering temperature would also be around 600 K. This is close to the recent report[52] of antiferromagnetic order above 500 K in $YBa_2Cu_3O_{6+\delta}$. Thus the very low susceptibility of oxides in which there is 180° Cu–O–Cu interactions may be understood in terms of a high antiferromagnetic ordering temperature.

The low magnetic susceptibility values in compounds with 180° Cu–O–Cu interactions is not likely to be due to the consequences of strong hybridization with oxide ions in single CuO_4 units as suggested by the MSXα calculations.[24] Li_2CuO_2 exhibits Curie–Weiss behavior with a Curie constant value close to that expected for an $S = {}^1/_2$ ion. This highlights the point that in accounting for the low susceptibility 180° Cu–O–Cu superexchange interactions are more important than the square-planar geometry of CuO_4 units. This is further supported by the fact that compounds in which the copper ions are in an isolated square-planar environment and also have small Cu–O distances show well-defined magnetic moments both from ESR and magnetic susceptibility studies as in the case of Bi_2CuO_4 and $La_{1.8}Ba_{1.2}Cu_{0.9}O_{4.8}$. In most of the cases where there are no 180° Cu–O–Cu interactions involving short Cu–O distances (~1.96 Å), the susceptibility is high and shows a strong temperature dependence. This is especially apparent in comparing the properties of Sr_2CuO_3 and $MgCu_2O_3$. Both of these compounds have chains of 180° Cu–O–Cu interactions. The former has a small, nearly temperature-independent susceptibility while in the latter the susceptibility is high and shows a strong temperature dependence. In the former, short Cu–O distances are involved along the chain while, in the latter, long Cu–O distances are involved. In $SrCuO_2$ the interchain 90° Cu–O–Cu interaction involving orthogonal orbitals between pairs of copper ions seems to have negligible influence on the dominant extended intrachain 180° Cu–O–Cu interaction. In $Ba_2Cu_3O_4Cl_2$, however, the strong temperature dependence of the susceptibility despite extended 180° Cu_A–O–Cu_A interactions shows the dominating influence of the Cu_B ions. In this compound the Cu^{2+} ions are involved in ferromagnetic 90° Cu_B–O–Cu_A interactions as well as antiferromagnetic 180° Cu_A–O–Cu_A interactions in the a–b plane. Thus there is a possibility of the magnetic interactions in this system being frustrated. Such a frustration may decrease the magnetic ordering temperature and cause the magnetic susceptibility to be relatively high.

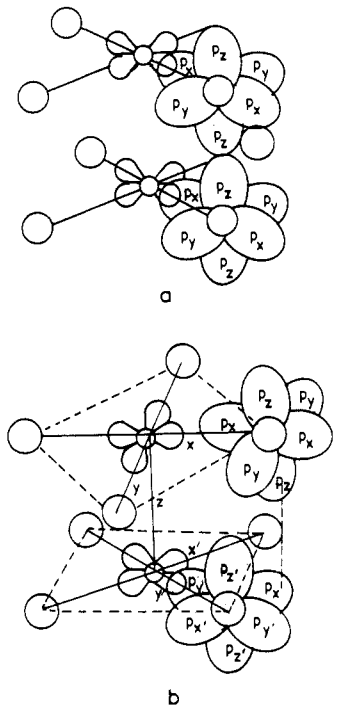

Figure 13. Schematic representation of the orbital interaction in square-planar geometry with (a) eclipsed and (b) staggered arrangement.

Cu–O–O–Cu Interaction. The interplanar interactions in La_2CuO_4 or those between the Cu_2 ions in $YBa_2Cu_3O_7$ involve Cu–O–O–Cu interactions. The magnitude of these interplanar transfer integrals relative to the intraplanar values may be important in determining the anisotropic Bose condensation temperatures. It is interesting to note that in these compounds where there is only Cu–O–O–Cu interaction, antiferromagnetic coupling becomes important around 30–50 K. This indicates that the Cu–O–O–Cu superexchange interaction is much weaker than the Cu–O–Cu superexchange interaction. This is comparable to the superconducting transition temperatures in the oxides derived from La_2CuO_4 or those derived from $YBa_2Cu_3O_{7-\delta}$ ($0.5 < \delta < 0.8$).

The sign of the Cu–O–O–Cu exchange interaction can depend on the geometry. When two square-planar CuO_4 units are stacked one on top of the other, one may anticipate antiferromagnetic interactions in an eclipsed geometry (involving nonorthogonal oxygen p orbitals, Figure 13a) and ferromagnetic interactions in a staggered geometry (involving orthogonal oxygen p orbitals, Figure 13b). The eclipsed geometry is seen, for example, along the b axis of Ca_2CuO_3, along the a axis of the Cu_1 ions in $YBa_2Cu_3O_7$, etc. In Bi_2CuO_4 the postulated singlet to triplet transition is consistent with its geometry. The situation in Y_2BaCuO_5 and $La_{1.8}Ba_{1.2}Cu_{0.9}O_{4.8}$ is also illustrative. Apparently the Cu–O–Cu interactions in the basal plane and along the c axis may have different exchange signs and magnitudes in these compounds.

Direct Cation–Cation Interactions. Direct Cu–Cu interactions that are not screened by intervening oxide ions are found in Bi_2CuO_4, Li_2CuO_2, $SrCuO_2$, Sr_2CuO_3, Ca_2CuO_3, $YBa_2Cu_3O_7$, etc. The shortest Cu–Cu distances are found in $SrCuO_2$, Li_2CuO_2, and Bi_2CuO_4, being 2.80, 2.84, and 2.92 Å, respectively. For Cu^{2+} (d^9) ions in square-planar coordination the d_{z^2} orbitals are filled and hence antiferromagnetic cation–cation interactions perpendicular to the CuO_4 square-planar units are not anticipated. However, this may not be valid when the copper ion is displaced from the plane of the oxygens (like the Cu_2 ions in Figure 1c). Direct cation–cation interaction between two half-filled $d_{x^2-y^2}$ orbitals across edge-shared CuO_4 units would be antiferromagnetic, as in the case of Li_2CuO_2.

The question of Coulombic repulsion between the two copper ions is important. It seems possible that the Coulombic repulsion

(48) (a) Wollan, E. O.; Child, H. R.; Koehler, W. C.; Wilkinson, M. K. *Phys. Rev.* **1958**, *112*, 1132. (b) Goodenough, J. B.; Longo, J. M.; In *Landolt-Börnstein, Physicalische und Chemische Tabellen*; Hellwege, K.-H., Ed.; Springer: West Berlin, 1970; Group III/4a, p 126.
(49) Kittel, C. *Introduction to Solid State Physics*, 6th ed.; Wiley: New York, 1986; p 445.
(50) Ganguly, P.; Rao, C. N. R. *Mater. Res. Bull.* **1973**, *8*, 405.
(51) Bosman, A. J.; van Daal, H. J. *Adv. Phys.* **1970**, *19*, 1.
(52) Tranquada, J. M.; Cox, D. E.; Kunmann, W.; Moudden, H.; Shirane, G.; Sueuaga, M.; Zolliker, P.; Valineu, D.; Siulia, S. K.; Alvery, M. S.; Jacobson, A.; Johnston, D. C. *Phys. Rev. Lett.* **1988**, *60*, 156.

between two copper ions with no intervening oxide ions (along the z axis) is minimized by the presence of a pair of electrons in the d_{z^2} orbitals. It has occurred to us that the coulomb repulsion energy in a chain of Cu^{2+} ions may be reduced to three-fourths if there is a disproportionation leading to an alternation of Cu^{+} and Cu^{3+} ions along the chain such as Cu_1^{1+}–Cu_2^{3+}–Cu_3^{1+}–Cu_4^{3+}···. For an isolated antiferromagnetically coupled ($S = 0$) Cu_A^{2+}–Cu_B^{2+} dimer, such a disproportionation can lead to two additional singlet states, Cu_A^{+}–Cu_B^{3+} and Cu_A^{3+}–Cu_B^{+}, assuming that the Cu^{3+} ion is in the low-spin state. These additional singlet states will be degenerate in the case of isolated dimers with equivalent copper sites. In a linear chain, however, the disproportionation may stabilize a charge density wave (CDW) in which there is an alternation of Cu^{+} and Cu^{3+}. Such a CDW would be further stabilized if there are two inequivalent copper sites favoring Cu^{+} and Cu^{3+} as is likely in the $I4$ symmetry of Bi_2CuO_4. The degeneracy of the two disproportionated states in the dimers would then be lifted, and one singlet state may become more stabilized compared to the other. The good fit to the susceptibility of Bi_2CuO_4 found with the factor of $^2/_3$ in the denominator in eq 2 instead of the factor of $^1/_3$ used in the classical Bleaney–Bowers expression suggests that one of the singlet states is much more stabilized compared to the other.[53] Such a disproportionation may be important for the unscreened –Cu_1–Cu_1–Cu_1– chains along the a axis of $YBa_2Cu_3O_7$.

Concluding Remarks

In this article we have studied a large number of ternary copper oxide systems having structural features common to the two known families of the high-temperature superconducting phases. The main conclusions that can be derived from these studies are as follows: (i) The magnitude and temperature dependence of the magnetic susceptibility are dependent more on the geometry of the extended copper–oxygen framework rather than the local geometry around the Cu^{2+} ion. (ii) While compounds with extended 180° Cu–O–Cu interactions show high antiferomagnetic interaction strength and low, nearly temperature-independent susceptibility, no ferromagnetic interaction was observed in compounds with 90° Cu–O–Cu superexchange interaction. (iii) Compounds in which Cu^{2+} ions are isolated with competing superexchange interactions show high temperature-dependent susceptibility. (iv) The Cu–O–O–Cu interaction (found between the planes of the oxide superconductors) is relatively weak compared with the Cu–O–Cu superexchange interaction. However, the antiferromagnetic coupling temperatures are close to the superconducting temperatures. The possibility of a disproportionation of Cu^{2+} to Cu^{+} and Cu^{3+} has been considered for the reduction of the magnetic moment observed in compounds such as Bi_2CuO_4 in which there exists direct Cu–Cu interaction. A puzzling result is that in the $La_2Ni_{1-x}Cu_xO_4$ system there is no contribution to the susceptibility from the Cu^{2+} ions even for small values of x.

Acknowledgment. We thank Professor C. N. R. Rao for encouragement and the University Grants Commission, New Delhi, India, for financial support.

Registry No. Ca_2CuO_3, 12213-78-4; Sr_2CuO_3, 12443-63-9; $Sr_2CuO_2Cl_2$, 57363-72-1; $Ba_2Cu_3O_4Cl_2$, 58206-72-7; Bi_2CuO_4, 39368-32-6; $La_{1.8}Ba_{1.2}Cu_{0.9}O_{4.8}$, 57608-96-5; $MgCu_2O_3$, 57608-96-5; $BaCuO_2$, 57348-58-0; $Y_2Cu_2O_5$, 12158-85-9; Li_2CuO_2, 12527-46-7; CuO, 1317-38-0; $CaCO_3$, 471-34-1; $Sr(NO_3)_2$, 10042-76-9; $SrCO_3$, 1633-05-2; $SrCl_2$, 10476-85-4; $BaCO_3$, 513-77-9; $BaCl_2$, 10361-37-2; Bi_2O_3, 1304-76-3; La_2O_3, 1312-81-8; $Ba(NO_3)_2$, 10022-31-8; $MgCO_3$, 546-93-0; Y_2O_3, 1314-36-9; LiOH, 1310-65-2; $Cu(NO_3)_2$, 3251-23-8.

(53) Sreedhar, K.; Ganguly, P.; Ramasesha, S. *J. Phys. C* **1988**, *21*, 1129.

Contribution from the Department of Chemistry, University of Alberta, Edmonton, Alberta, Canada T6G 2G2

Synthesis and Structure of a Diphosphetene, $(CF_3)\overline{P(CF_3)PC(SiMe_3)=C(SiMe_3)}$, and the Coordination and Metallacycle Formation of Several Diphosphetenes with Iridium(I)

Ian G. Phillips, Richard G. Ball, and Ronald G. Cavell*

Received September 25, 1987

New diphosphetenes $(CF_3)\overline{P(CF_3)PC(R)=C(R')}$, **9** (R = R′ = $SiMe_3$), **10** (R = R′ = Ph), and **11** (R = CH_3, R′ = $SiMe_3$), have been prepared by the reaction of $(CF_3P)_{4,5}$ and the appropriate alkyne. The first of these has been structurally characterized. For **9** at −65 °C (monoclinic $C2/c$, No. 15): a = 17.057 Å, b = 8.811 Å, c = 11.983 Å, β = 102.13°, and Z = 4. The central P_2C_2 ring is slightly twisted from planarity (the angle between the PP vector and the CC vector is 12.8°). Major bond lengths are P–P = 2.223 (1) Å, P–C_{endo} = 1.841 (2) Å, and C–C = 1.356 (3) Å. The new diphosphetenes **10** and **11** and also $(CF_3)\overline{P(CF_3)PC(CF_3)=C(CF_3)}$ (**1**) (prepared in 1964 by W. Mahler) react with *trans*-$[IrCl(N_2)(PPh_3)_2]$ at low temperature to form an η^1 (phosphorus) complex, which transforms to a metallacycle with the

framework at ordinary temperatures. NMR spectral properties of the diphosphetenes, the η^1 complexes, and the metallacycles are given.

Introduction

In 1964 Mahler[1] reported the synthesis and characterization of the first 1,2-diphosphetene (**1**) and the 1,2,3-triphospholene (**2**) by copyrolysis of $[CF_3P]_{4,5}$ with excess hexafluorobut-2-yne at 170 °C (eq 1, R = R′ = CF_3, 170 °C, 3 days). Heating $[(CF_3)P]_{4,5}$ with $CH_3C{\equiv}CCH_3$ under similar conditions produced a triphospholene $(CF_3)\overline{P(CF_3)P(CF_3)PC(CH_3)=C(CH_3)}$ (**3**), which was characterized by its NMR spectra, but no corresponding diphosphetene was obtained.[2] Reinvestigation of the pyrolysis of $[PhP]_5$ with PhC≡CPh (a reaction first reported by Ecker and Schmidt[3] in 1973) by Mathey et al.[4,5] showed that the scope of this preparative route could be broadened. Improved yields and alternative synthesis of other diphosphetenes and tri-

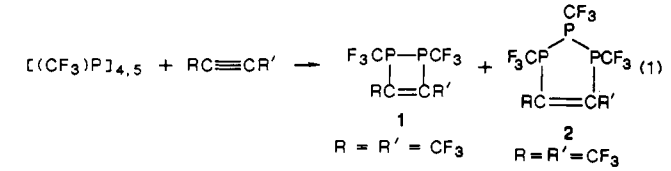

(1) Mahler, W. *J. Am. Chem. Soc.* **1964**, *86*, 2306.

(2) Mahler, W., personal communication 1986.
(3) Ecker, A.; Schmidt, U. *Chem. Ber.* **1973**, *106*, 1453.
(4) Charrier, C.; Guilhem, J.; Mathey, F. *J. Org. Chem.* **1981**, *46*, 3.
(5) Charrier, C.; Margiot, N.; Mathey, F.; Robert, F.; Jeannin, Y. *Organometallics* **1986**, *5*, 623.

0020-1669/88/1327-2269$01.50/0